Can tailored non-linearity of hierarchical structures inform future material development?

Matthew P. O'Donnell[a,*], Paul M. Weaver[a], Alberto Pirrera[a]

[a] *ACCIS, Queen's Building, University of Bristol, Bristol UK, BS8 1TR*

Abstract

An analytical investigation into the non-linear elastic response of helical lattice structures coupled with an elastic medium is presented. Novel composite templates are then obtained to produce bespoke material characteristics by exploiting tuned hierarchy. System behaviour is approximated as a combination of three non-linear "springs", representing the helical lattice, and the axial and circumferential components of the elastic medium via an energy based approach. Non-dimensional parameters governing each component's non-linear load-displacement behaviour are identified, demonstrating tailoring potential. Further tunable parameters that govern the combined system response, involving form factor, geometric and stiffness ratios are identified. In particular, pseudo-ductile responses are observed. The feasible region of pseudo-ductility, as determined by these non-dimensional parameters, is obtained, allowing discussion of viable materials and geometries. Finally, load-displacement behaviour is utilised to obtain indicative effective stress-strain curves, thus showing promise as a model for future material development.

Keywords: Pseudo-Ductility, Analytical Modelling, Non-Linear Elasticity, Hierarchical Structures.

1. Introduction

Structures that present non-linear elastic responses to applied loading have the potential to offer predictable, repeatable, load-displacement behaviour that has favourable characteristics. We describe how a hierarchical structure composed of a helical lattice and elastic medium can be successfully tuned to achieve a set of desired characteristics. In general, the resulting behaviour may be tuned to a variety of responses, however, to highlight one such possibility, we focus on the introduction of pseudo-ductile qualities in the resulting system's elastic stress-strain response. As there is no universally accepted definition of pseudo-ductility, herein, we describe pseudo-ductile systems as those that possess characteristics that mimic the key features of a traditional ductile material via non-linear elasticity, e.g. a softening of the effective modulus following an initially positive region.

*Corresponding Author: Matt.ODonnell@bristol.ac.uk

Many mechanisms for introducing ductile-like qualities into composite components have been proposed and are often reliant upon plastic deformations and damage mechanisms [1–7], with the inherent limitation of causing non-recoverable loss of stiffness/performance. Non-linear elastic behaviour offers a clear benefit as an alternative by providing repeatable deformations.

As is often observed in biological systems, structural hierarchy offers potential mechanisms to achieve novel material characteristics [8–10]. In the composite system presented—itself inspired by the virus bacteriophage T4 [11]—the reinforcement comprises a helical lattice that is itself constructed from composite strips. This lattice is subsequently infiltrated with an elastic medium forming a hierarchical system. The phases are referred to within as the 'helical lattice' and 'elastic medium', respectively. Hierarchy is observed at the length scale of the fibre/matrix, defining the helical strip's overall stiffness properties. At the laminate scale the anisotropy of the composite strips is exploited in order to tune the response characteristics of the helical lattice in conjunction with the elastic medium's properties. Recent investigations into the behaviour of similar helical structures, using lattices, ribbons, and ladder-like geometries demonstrate the huge potential for tuning non-linear responses [11–13]. It is anticipated that the proven bistability of some helical lattices, and the effective negative stiffness they produce, may be aligned antagonistically to the elastic medium in order to produce the required pseudo-ductile qualities.

Herein, an energy based model for the helical lattice developed by Pirrera *et al.* [11] is extended to include the effects of the elastic medium. The additional components are included in the energy formulation as effective axial and circumferential springs. The simplifying assumption in the analytical model, i.e. the investigation of an equivalent "three-spring" system, allows for a straightforward representation of the underlying physics that could, in future works, be applied to micro-braided lattice structures. Using this modelling approach insight into the required stiffness, geometry and form factors of such systems can be obtained. In identifying how the hierarchical properties of the system must be tuned to achieve desired pseudo-ductile behaviour we are able to inform the development of future pseudo-ductile composites materials. In general, through exploiting composite hierarchy in this manner it is possible to produce systems that offer bespoke material characteristics providing significant opportunities for improved design.

We proceed with the development of the underlying analytical model. Key non-dimensional parameters governing the nature of the response are identified and examples of the predicted behaviour presented. Finally, regions of pseudo-ductile feasibility are identified in terms of these non-dimensional parameters.

2. Energy Based Analysis

Pirrera *et al.* developed an energy based formulation for the helical lattice where individual helices are considered as inextensional strips that lie upon the surface of a cylinder [11]. The strips are sufficiently narrow that the behaviour across the width can be ignored. Furthermore, the hinge points in the lattice

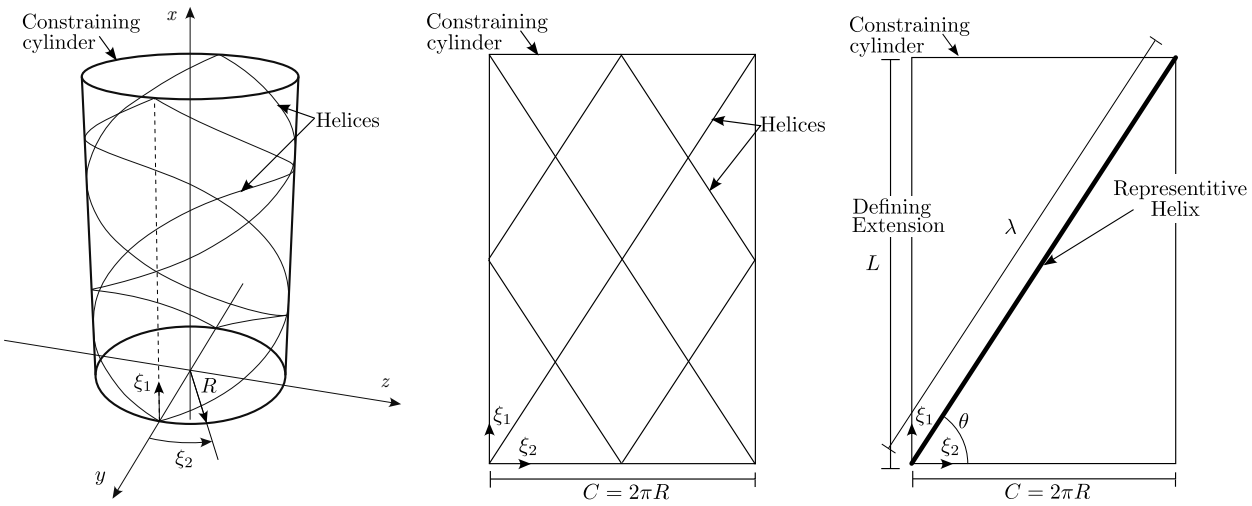

(a) Sketch of a cylindrical lattice. (b) Planar projection of lattice. (c) Representative helix.

Figure 1: Sketch of a typical lattice comprised of four helical strips on the surface of its constraining cylinder and its planar representation. The simplified unit cell shows the equivalent single helix arising due to the assumptions made, namely the mirror symmetric arrangement and common pitch angle. Additionally the extension, L, can then be used as the defining variable.

structure remain fixed such that individual helices do not slide over each other but together can translate in space. If a further condition is imposed on the helical lattice, that of mirror-symmetric reinforcing strips with a common pitch angle, there is no lattice twist under extension. Under these assumptions the deformations observed for any right or left handed helical strip are mirrored and the choice of a mirror symmetric layup, therefore, permits the use of a single representative helix as all strips are energetically equivalent. Utilising a single representative helix permits a simplification of the unit cell allowing extension, rather than the radial diameter, to characterise behaviour, thus permitting a more direct analysis of the load-extension behaviour [11]. The cylindrical helical lattice structure is represented on the plane by reference to its simplified unit cell, Figure 1.

It is noted that we maintain the use of the expression 'unit cell' for continuity with Pirrera *et al.* [11], but for modelling purposes in this analysis it refers to a full representative helix. The total volume enclosed by the helices is assumed to be minimal and so does not impact the ability to include the elastic medium.

Figure 2 shows a representative unit cell for the system including the axial and circumferential springs used to describe the behaviour of the elastic medium. The system's geometric configuration can be completely defined by its axial length, $L \in [0, \lambda]$. When $L = 0$ the system is in a fully coiled state with $L = \lambda$ representing the completely extended state. Alternatively the extension can be described using a

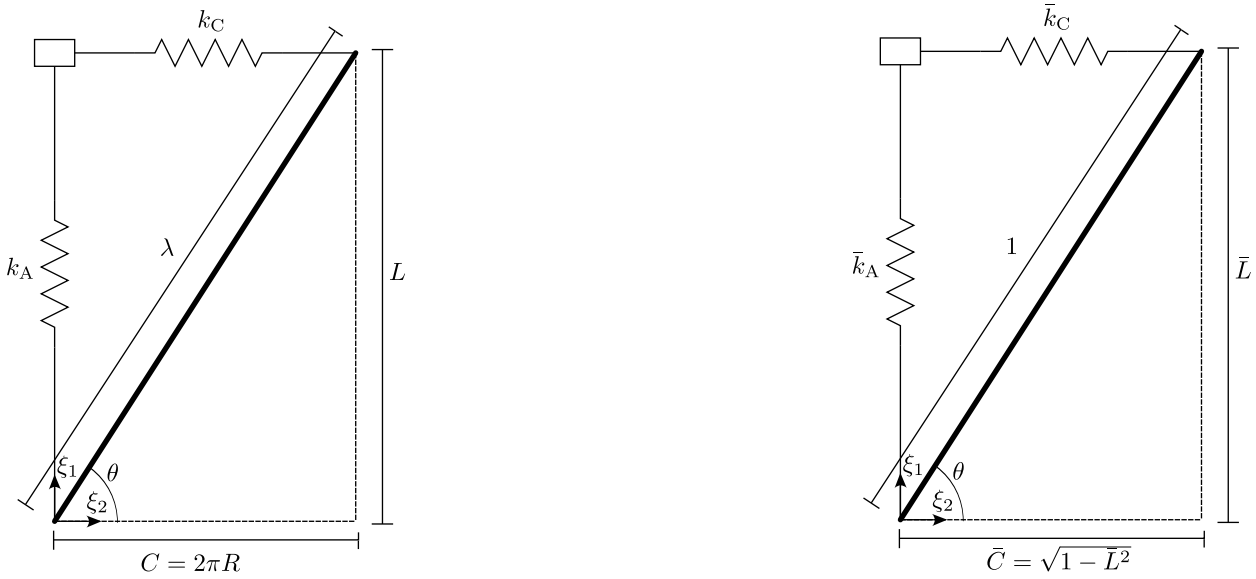

(a) Sketch of the unit cell.

(b) Non-dimensionalised geometry.

Figure 2: Illustration of the unit cell composed of two elastic springs and the lattice together with the equivalent non-dimensional system.

non-dimensional quantity,[1]

$$\bar{L} = \frac{L}{\lambda}, \qquad \bar{L} \in [0, 1]. \tag{1}$$

The extension of a typical lattice structure is illustrated further in Figure 3, as reproduced from Pirrera *et al.* demonstrating the bistable behaviour [11].

The total internal energy, U, can be described as a linear combination of three spring-like energy components: the helical lattice structure, U_H, the axial component of the elastic medium, U_A, and the circumferential component, U_C. The internal energy together with the work done, V, by an external force, F,

[1] Non-dimensional quantities are indicated by an over-bar throughout.

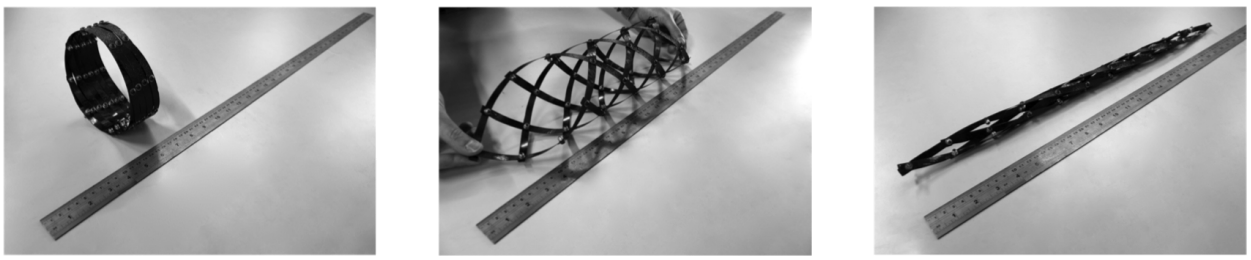

(a) Fully coiled state $\bar{L} \to 0$.

(b) Partial extension $\bar{L} \in (0, 1)$.

(c) Fully extended state $\bar{L} \to 1$.

Figure 3: Examples of a helical lattice structure in various states of extension - reproduced from Pirrera *et al.* [11]. The system is in a position of instability in 3b and spontaneously extends or contracts to stable states 3a and 3c.

displacing the structure from its equilibrium position, L_{E}, can be expressed as

$$U = U_{\mathrm{H}}(L) + U_{\mathrm{A}}(L) + U_{\mathrm{C}}(L), \qquad V(L) = -F(L - L_{\mathrm{E}}), \tag{2}$$

allowing the total potential energy of the system, $\Pi = U + V$, to be defined. Π has stationary points that may be obtained from the solution of

$$\frac{d\Pi}{dL} = \frac{dU_{\mathrm{H}}}{dL} + \frac{dU_{\mathrm{A}}}{dL} + \frac{dU_{\mathrm{C}}}{dL} + \frac{dV}{dL} = 0. \tag{3}$$

In order to obtain the force-displacement behaviour equation (3) can be expressed as

$$F = \frac{dU_{\mathrm{H}}}{dL} + \frac{dU_{\mathrm{A}}}{dL} + \frac{dU_{\mathrm{C}}}{dL} = \frac{dU}{dL}. \tag{4}$$

As such we concern ourselves with the behaviour of each of the derivatives in equation (4). We discuss the behaviour of each component individually in order to explore potential trends in non-linearity. Knowledge of each component is then used to guide further study into the combined behaviour to meet the objective of identifying pseudo-ductile responses.

2.1. Lattice Behaviour

Each lattice strip has an identical stiffness, pre-curvature and initial pitch angle for all right handed helices and is mirrored for left handed ones. Put simply, the internal energy, U_{H}, of a strip of area A can be determined from Classical Laminate Theory (CLT) [14],

$$U_{\mathrm{H}} = \frac{1}{2} \int_A \Delta\boldsymbol{\kappa}^T \mathbf{d} \Delta\boldsymbol{\kappa} \, dA, \tag{5}$$

where we consider only the axial and twist components of curvature, $\boldsymbol{\kappa}(L)$, and pre-curvature, $\boldsymbol{\kappa}_0$,

$$\boldsymbol{\kappa}(L) = \begin{bmatrix} \kappa_x \\ \kappa_{xy} \end{bmatrix}, \qquad \boldsymbol{\kappa_0} = \begin{bmatrix} \kappa_{x0} \\ \kappa_{xy0} \end{bmatrix}, \qquad \Delta\boldsymbol{\kappa} = \boldsymbol{\kappa}(L) - \boldsymbol{\kappa_0} = \begin{bmatrix} \kappa_x - \kappa_{x0} \\ \kappa_{xy} - \kappa_{xy0} \end{bmatrix}, \tag{6}$$

together with the corresponding terms of the reduced bending stiffness matrix, $\mathbf{d}$,

$$\mathbf{d} = \begin{bmatrix} d_{11} & d_{16} \\ d_{16} & d_{66} \end{bmatrix}, \qquad \mathbf{d} = \mathbf{D} - \mathbf{B}\mathbf{A}^{-1}\mathbf{B}, \tag{7}$$

with $\mathbf{A}$, $\mathbf{B}$, and $\mathbf{D}$ the usual extensional, coupling and flexural stiffness matrices as defined in CLT [14].

The pre-curvature, $\boldsymbol{\kappa}_0$, is the unstressed state of the strips following cure, i.e. its cured shape. The additional curvatures, $\boldsymbol{\kappa}$, are associated with assembling the strips to conform to the helical lattice's geometry and subsequent deformations of the helical lattice. For example, if the strips were cured as a flat strip they would have zero pre-curvature, but there would be an associated energy in deforming them to conform to the helical lattice's geometry and, therefore, the helical lattice would possess no zero energy state.

Referring to the description of the unit cell with diagonal length λ (Figure 2), a lattice composed of N strips of width W can then be described by formulating the curvature using the Weingarten map, which can be specified in terms of one variable, $\bar{L}$ [11]. The energy of the helical lattice is given in terms of non-dimensional parameters,

$$U_{\mathrm{H}} = d_{11} \overbrace{\frac{2\pi^2 NW}{\lambda}}^{\alpha_{\mathrm{H}}} \overbrace{\left\{\Delta\bar{\boldsymbol{\kappa}}^T \bar{\mathbf{d}} \Delta\bar{\boldsymbol{\kappa}}\right\}}^{\bar{U}_{\mathrm{H}}} = d_{11}\alpha_{\mathrm{H}}\bar{U}_{\mathrm{H}}, \tag{8}$$

where

$$\Delta\boldsymbol{\kappa} = \frac{2\pi}{\lambda}\Delta\bar{\boldsymbol{\kappa}} = \frac{2\pi}{\lambda}\begin{bmatrix}\sqrt{1-\bar{L}^2} - \bar{\kappa}_{x0} \\ \bar{L} - \bar{\kappa}_{xy0}\end{bmatrix}, \qquad \boldsymbol{\kappa}_0 = \frac{2\pi}{\lambda}\bar{\boldsymbol{\kappa}}_0, \qquad \mathbf{d} = d_{11}\boldsymbol{\delta}, \tag{9}$$

with

$$\boldsymbol{\delta} = \begin{bmatrix}1 & \delta_{16} \\ \delta_{16} & \delta_{66}\end{bmatrix}, \qquad \delta_{16} = \frac{d_{16}}{d_{11}}, \qquad \delta_{66} = \frac{d_{66}}{d_{11}}. \tag{10}$$

Expanding the multiplication gives the non-dimensional helical lattice energy $\bar{U}_{\mathrm{H}}$

$$\bar{U}_{\mathrm{H}} = \left(\sqrt{1-\bar{L}^2} - \bar{\kappa}_{x0}\right)^2 + 2\delta_{16}\left(\sqrt{1-\bar{L}^2} - \bar{\kappa}_{x0}\right)\left(\bar{L} - \bar{\kappa}_{xy0}\right) + \delta_{66}\left(\bar{L} - \bar{\kappa}_{xy0}\right)^2, \tag{11}$$

and its derivative with respect to $\bar{L}$

$$\frac{1}{2}\frac{d\bar{U}_{\mathrm{H}}}{d\bar{L}} = (\delta_{66}-1)\,\bar{L} + \delta_{16}\frac{1-2\bar{L}^2}{\sqrt{1-\bar{L}^2}} + \bar{\kappa}_{x0}\left(\frac{\bar{L}}{\sqrt{1-\bar{L}^2}} - \delta_{16}\right) + \bar{\kappa}_{xy0}\left(\delta_{16}\frac{\bar{L}}{\sqrt{1-\bar{L}^2}} - \delta_{66}\right). \tag{12}$$

Equation (12) indicates how the non-dimensional stiffness properties, $\boldsymbol{\delta}$, and pre-curvatures, $\bar{\boldsymbol{\kappa}}_0$, can be altered to affect significant changes in the helix's non-linear response. Equation (4) gives the relationship between force and the derivatives of each component of internal energy. For the case of the helical lattice in isolation it reduces to,

$$F = \frac{dU_{\mathrm{H}}}{dL} = \frac{d_{11}}{\lambda}\alpha_{\mathrm{H}}\frac{d\bar{U}_{\mathrm{H}}}{d\bar{L}}(\bar{L}), \tag{13}$$

or in its equivalent non-dimensional form

$$\bar{F} = \frac{d\bar{U}}{d\bar{L}} = \frac{d\bar{U}_H}{d\bar{L}}. \tag{14}$$

It is therefore sufficient to consider the behaviour of the non-dimensional energy in order to understand the helix's non-linear response. The root(s) of equation (12), $\bar{L}_{\mathrm{E}}$, give the unloaded equilibrium position of the system with the sign of the slope determining the stability. The slope itself can be interpreted as the effective stiffness of the system; for example a positive slope indicates a stable equilibrium point and the gradient of which corresponds to the positive non-dimensional stiffness. Alternatively, a negative slope indicates an unstable equilibrium point, and in effect a negative stiffness. For negative stiffness structures, additional stable points are observed at the end of the domain $\bar{L} = [0, 1]$, as the system cannot displace any further. The change in length of the system, $\Delta\bar{L} = \bar{L} - \bar{L}_{\mathrm{E}}$, can be defined relative to each equilibrium position, $\bar{L}_{\mathrm{E}}$, allowing comparison of various systems effective stiffness.

2.2. Elastic Medium

The elastic medium is assumed to behave like two springs with the force varying linearly with changes in circumferential and axial displacements. This approximation, i.e. ignoring bulk effects, allows the model to be greatly simplified, whilst still capturing underlying physical behaviour. The axial and circumferential springs possesses stiffness k_{A} and k_{C}, respectively. These are calculated assuming the thickness of the elastic medium, H, is much smaller than the radius of the helical lattice, i.e. $H \ll R$,

$$k_{\mathrm{A}} = \frac{EH\bar{\mathrm{C}}_0}{\bar{L}_0}, \qquad\qquad k_{\mathrm{C}} = \frac{EH\bar{L}_0}{\bar{\mathrm{C}}_0}. \tag{15}$$

The effective spring stiffness is calculated using the Young's modulus, E, of the elastic medium, and $\bar{L}_0$ and $\bar{\mathrm{C}}_0$, correspond to the initial zeroed position of the springs. Referring to the unit cell in Figure 2, $\bar{L}_0$ defines $\bar{\mathrm{C}}_0$. The zeroed spring position for the elastic medium need not correspond to the equilibrium position, $\bar{L}_{\mathrm{E}}$, of the combined helix-medium system, i.e. the helix could first be assembled and then embedded in the elastic medium while held at a pre-defined extension. Varying $\bar{L}_0$ allows for additional tailoring, in a similar manner to varying the pre-curvature, $\bar{\boldsymbol{\kappa}}_{\mathbf{0}}$, of the helical strips, and can be tuned for differing behaviours.

The energies associated with each elastic medium spring can then be defined from the change in length, ΔL, and circumference, ΔC, respectively,

$$U_{\mathrm{A}} = \frac{1}{2}k_{\mathrm{A}}(\Delta L)^2, \qquad\qquad U_{\mathrm{C}} = \frac{1}{2}k_{\mathrm{C}}(\Delta C)^2, \tag{16}$$

or, equivalently,

$$\begin{aligned} U_{\mathrm{A}} &= d_{11}\overbrace{\frac{1}{2}\frac{E\lambda^3}{d_{11}}\frac{\mathrm{H}}{\lambda}}^{\alpha_{\mathrm{M}}}\overbrace{\left\{\frac{\sqrt{1-\bar{L}_0^2}}{\bar{L}_0}\left(\bar{L}-\bar{L}_0\right)^2\right\}}^{\bar{U}_{\mathrm{A}}} = d_{11}\alpha_{\mathrm{M}}\bar{U}_{\mathrm{A}}, \\ U_{\mathrm{C}} &= d_{11}\frac{1}{2}\frac{E\lambda^3}{d_{11}}\frac{\mathrm{H}}{\lambda}\underbrace{\left\{\frac{\bar{L}_0}{\sqrt{1-\bar{L}_0^2}}\left(\sqrt{1-\bar{L}^2}-\sqrt{1-\bar{L}_0^2}\right)^2\right\}}_{\bar{U}_{\mathrm{H}}} = d_{11}\alpha_{\mathrm{M}}\bar{U}_{\mathrm{H}}, \end{aligned} \tag{17}$$

where

$$\Delta\bar{L} = \bar{L} - \bar{L}_0 \qquad\qquad \Delta\bar{C} = \bar{C} - \bar{C}_0 = \sqrt{1-\bar{L}^2} - \sqrt{1-\bar{L}_0^2}, \tag{18}$$

with the change in circumference obtained by application of Pythagoras' theorem, Figure 2.

The derivatives with respect to $\bar{L}$ are

$$\frac{1}{2}\frac{d\bar{U}_{\mathrm{A}}}{d\bar{L}} = \frac{\sqrt{1-\bar{L}_0^2}}{\bar{L}_0}(\bar{L}-\bar{L}_0), \qquad \frac{d\bar{U}_{\mathrm{C}}}{d\bar{L}} = \frac{\bar{L}_0}{\sqrt{1-\bar{L}_0^2}}\frac{-\bar{L}}{\sqrt{1-\bar{L}^2}}\left(\sqrt{1-\bar{L}^2}-\sqrt{1-\bar{L}_0^2}\right). \tag{19}$$

2.3. Combined Helix-Medium System Behaviour

The non-dimensional energy of the helical lattice and the elastic medium have been investigated individually. The combined behaviour is given by,

$$\frac{dU}{dL} = \frac{d_{11}}{\lambda}\left(\alpha_{\mathrm{H}}\frac{d\bar{U}_{\mathrm{H}}}{d\bar{L}} + \alpha_{\mathrm{M}}\left(\frac{d\bar{U}_{\mathrm{A}}}{d\bar{L}} + \frac{d\bar{U}_{\mathrm{C}}}{d\bar{L}}\right)\right). \tag{20}$$

The relative magnitudes of each component is determined by the non-dimensional multiplication coefficients α_{H} and α_{M}, and their ratio α_{Π}

$$\alpha_{\mathrm{H}} = 2\pi^2 N\frac{W}{\lambda}, \qquad \alpha_{\mathrm{M}} = \frac{1}{2}\frac{E\lambda^3}{d_{11}}\frac{\mathrm{H}}{\lambda}, \qquad \alpha_{\Pi} = \frac{\alpha_{\mathrm{M}}}{\alpha_{\mathrm{H}}} = \frac{1}{4\pi^2 N}\,\frac{E\lambda^3}{d_{11}}\,\frac{\mathrm{H}}{W}, \tag{21}$$

allowing the total energy to be expressed compactly as,

$$\frac{dU}{dL} = \frac{d_{11}}{\lambda}\alpha_{\mathrm{H}}\overbrace{\left\{\frac{d\bar{U}_{\mathrm{H}}}{d\bar{L}} + \alpha_{\Pi}\left(\frac{d\bar{U}_{\mathrm{A}}}{d\bar{L}} + \frac{d\bar{U}_{\mathrm{C}}}{d\bar{L}}\right)\right\}}^{\frac{d\bar{U}}{d\bar{L}}} = \frac{d_{11}}{\lambda}\alpha_{\mathrm{H}}\frac{d\bar{U}}{d\bar{L}}. \tag{22}$$

For a given system, α_{Π}, governs the relative magnitudes of the helical lattice and elastic medium dictating the nature of the response. The results of varying this parameter is investigated following the definition of effective strain for the system.

3. Tuning Non-Linear Behaviour

3.1. Effective Strain of the System

In order to evaluate the stress-strain response an effective strain for the hierarchical system must be defined. While the elastic medium is assumed to experience in-plane deformation, the helical lattice's strips are assumed to be inextensional. A global effective strain of the structure can be defined in terms of extension from the equilibrium position, $\bar{L}_{\mathrm{E}}$, to the final length, $\bar{L}$. This can be expressed in terms of non-dimensional parameters as

$$\varepsilon = \frac{\Delta\bar{L}}{\bar{L}_{\mathrm{E}}} = \frac{\bar{L}}{\bar{L}_{\mathrm{E}}} - 1, \tag{23}$$

where $\bar{L}_{\mathrm{E}} \in [0, 1]$. Although the range of structural displacements is bounded, $\bar{L} \in [0, 1]$, the initial equilibrium position, $\bar{L}_{\mathrm{E}}$, has a significant impact on the magnitude of the effective strains observed. For the multi-stable systems there can be more than one value for $\bar{L}_{\mathrm{E}}$. However, by limiting the analysis to systems that possess pseudo-ductile responses there is a stable equilibrium point that can be taken as the reference value. In this analysis we restrict ourselves to curves which possess a single stable equilibrium point within the domain, i.e. $\bar{L}_{\mathrm{E}} \in (0, 1)$.[2]

[2]Excluding the possibility of stable positions at the end points $\bar{L} = [0, 1]$ as previously discussed.

Table 1: Properties of an example configuration.

$\bar{L}_0$	δ_{16}	δ_{66}	$\bar{\boldsymbol{\kappa}}_{\mathbf{0}}$
0.3	0.334	0.166	**0**
0.4	0.334	0.166	**0**

3.2. Pseudo-Ductile Response

A typical set of system properties is investigated (Table 1) that were selected to minimise the number of variables under consideration. For this particular system's configuration the behaviour for varying α_Π can be investigated for two spring equilibrium positions $\bar{L}_0 = \{0.3, 0.4\}$. The family of curves in Figure 4 have negative gradient until α_Π rises above a specified threshold and are not shown as they do not possess a stable equilibrium position within the domain and, therefore, lack the required pseudo-ductility. Below the pseudo-ductility threshold the negative stiffness of the helix dominates the system's behaviour. Increasing α_Π permits an increased contribution of the elastic medium until an approximately linear profile is observed. It must be noted that this approximately linear behaviour, as illustrated by the difference between the continuous and dashed lines in Figure 4, may only be observed in the earlier stages of deformation in Figures 4b and 4b. The deviation of the continuous curves from the reference dashed lines, representing the initial modulus, shows a reduction of effective stiffness. As α_Π increases, there is no longer an observable region of reduced stiffness that characterises a pseudo-ductile response. The pseudo-ductile plateau diminishes as the elastic medium completely dominates behaviour. The exact point at which ductility diminishes is not clearly defined and an appropriate judgement was made to include the full range from the onset of pseudo-ductility to an approximately linear initial response. Quantifying the pseudo-ductility of these responses, and determining more exact bounds for the feasible regions, could be conducted in the future.

In the configurations investigated, pseudo-ductile behaviour is observed upon extension of the system from its initial equilibrium position, $\bar{L} = \bar{L}_\mathrm{E} \in (0, 1)$, towards a nearly fully extended state, $\bar{L} \to 1$. Due to the definition of strain, as given in equation (23), if the initial equilibrium position is not close to the fully extended state, such that for instance $\bar{L}_\mathrm{E} \lesssim 0.91$, then large effective strains are observed. This behaviour explains the relatively large strains observed in Figure 4. As evident in Figure 4c, with $\bar{L}_0 = 0.4$ and $\alpha_\Pi = 0.75$, the system can be tuned to minimise the strain at the peak of the plateau via a suitable choice of $\bar{L}_\mathrm{E}$. However, this approach simultaneously reduces the effective modulus value. By tuning the system parameters in Table 1, along with α_Π, improved behaviour may be obtained. Simultaneously establishing the optimal parameters of the helix and medium is beyond the scope of this study but the potential for further investigation is evident.

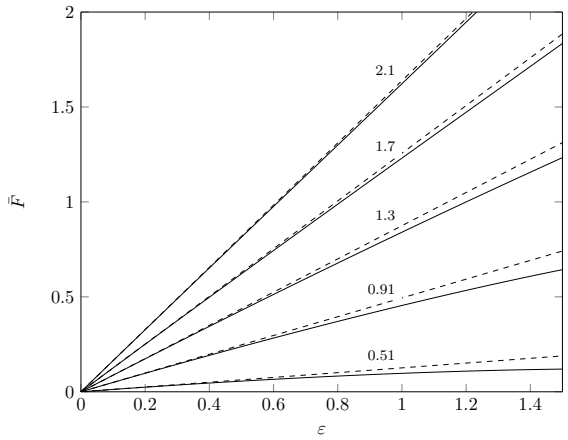

(a) Pseudo-ductile responses of helix-medium system for changes in α_Π for $L_0 = 0.3$.

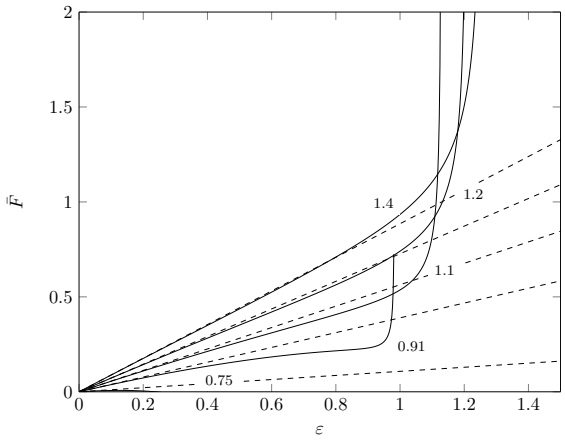

(b) Pseudo-ductile responses of helix-medium system for changes in α_Π for $L_0 = 0.4$.

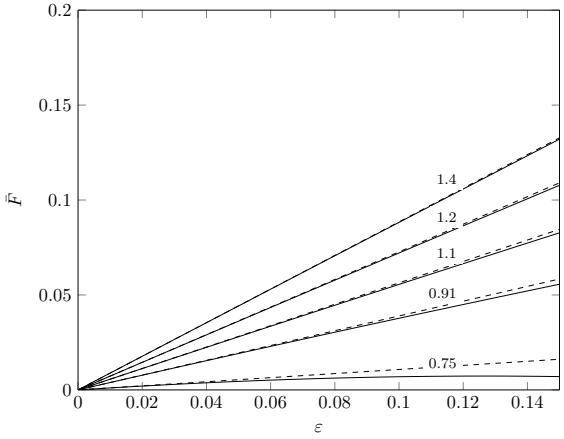

(c) Example of the initial stages of response for curves drawn in figure 4b with changes in α_Π for $L_0 = 0.4$.

Figure 4: Identification of pseudo-ductile responses of helix-medium system as determined by parameter α_Π. Initial modulus (dashed lines) is provided for comparison.

3.3. Effective Stress of the System

In order to obtain an *effective material* stress-strain response we seek to define an appropriate measure for stress. In typical applications it is sufficient to assume that the applied load is distributed over the initial cross sectional area. However, due to the large variation in radius from the fully coiled to fully extended state the cross sectional area of the combined structure exhibits significant variations. In order to define the effective stress assumptions a definition of the effective area must be made.

In order to define the effective area of the elastic medium, used in calculating the effective spring stiffness, the following area was utilised,

$$A_0 = \lambda H \sqrt{1 - \bar{L}_0^2}. \tag{24}$$

Alternatively, we can define a variable cross-sectional area,

$$A_{\mathrm{A}} = \lambda H \sqrt{1 - \bar{L}_0} \frac{\bar{L}_0}{\bar{L}}, \tag{25}$$

with $R \gg H$ and a constant elastic material volume distributed along the length, noting that large changes of the radius of annulus occurs. Both of these areas can define the effective stress of the system, the effect of which is now explored. By substituting the appropriate area the stresses, σ_0, and σ_{A}, may be defined as,

$$\sigma_0 = \frac{E}{2\alpha_\Pi} \frac{1}{\sqrt{1 - \bar{L}_0^2}} \frac{d\bar{U}}{d\bar{L}}, \qquad \sigma_{\mathrm{A}} = \frac{E}{2\alpha_\Pi} \frac{1}{\sqrt{1 - \bar{L}_0^2}} \frac{\bar{L}}{\bar{L}_0} \frac{d\bar{U}}{d\bar{L}}, \tag{26}$$

assuming a constant and variable cross-sectional area, respectively. These two definitions illustrate the differences in behaviour sufficiently and further area definitions are not be explored.

In order to obtain dimensional stress-strain curves, as seen in Figure 5, a nominal value of $E = 1$ GPa is used together with the corresponding non-dimensional curves identified in Figure 4a (with various α_Π and $\bar{L}_0 = 0.3$). Inspection of equation (26) indicates that the stress is linearly proportional to the elastic medium's stiffness E, as such the choice of $E = 1$ GPa can readily be interpreted for other stiffness values. For the case of constant area, A_0, the modulus retains the desired property of softening at increased strains. However, as is evident in Figure 5b, the changing area, A_{A}, results in an initially increasing modulus but still retains the pseudo-ductile plateau for $\alpha_\Pi = 0.91$. These results indicate how non-linearities in the response can be tailored significantly to achieve desirable characteristics. The divergence of the stress-strain curves observed in Figure 5 can be explained by considering equations (12) and (19) where singularities in force-displacement response are predicted as the extension approaches $\bar{L} = 1$. The sign of this divergence is dictated by the dominating feature in the combined system, in the case of a positive divergence the elastic medium dominates behaviour, whereas in the case of negative divergence the negative stiffness of the helical lattice is the more significant component. It is noted, in a fully extended physical system, approaching

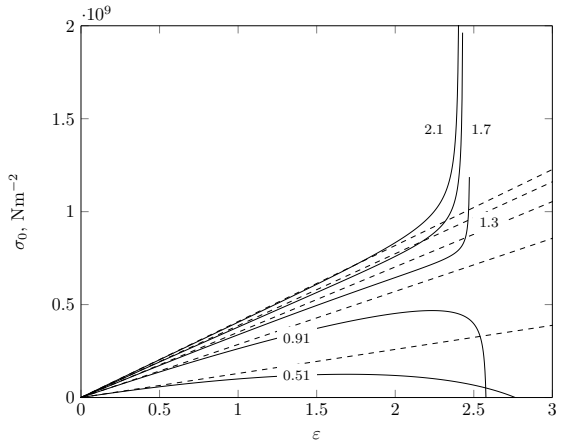

(a) Effective stress as calculated using σ_0, for various α_Π with $\bar{L}_0 = 0.3$.

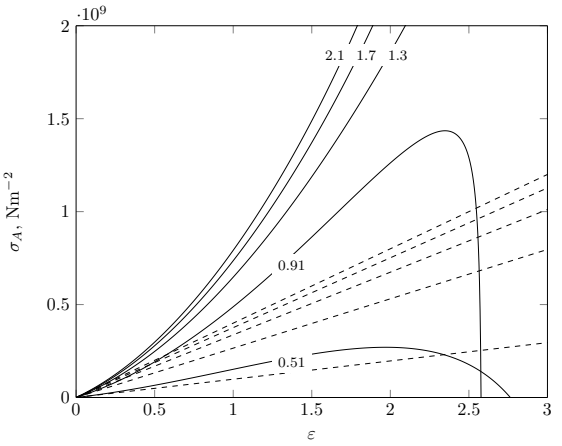

(b) Effective stress as calculated using σ_{A}, for various α_Π with $\bar{L}_0 = 0.3$.

Figure 5: Comparison of the effective stress measures for an elastic medium of stiffness $E = 1$ GPa displaying various levels of ductility and peak stress. Non-dimensional force taken from Figure 4a. Initial modulus (dashed lines) is provided for reference.

$\bar{L} = 1$, self intersection of the constituent parts influences the behaviour before the predicted divergence occur.

The following section discusses how the form-factor, geometric and stiffness characteristics of the system must be carefully balanced in order to achieve feasible α_Π values.

4. Configuring a Pseudo-Ductile System

Insight into pseudo-ductile responses can be drawn from the three non-dimensional components that make up α_Π,

$$\alpha_\Pi = \frac{\alpha_{\mathrm{M}}}{\alpha_{\mathrm{H}}} = \overbrace{\frac{1}{4\pi^2 N}}^{(\beta_{\mathrm{F}})} \overbrace{\frac{E\lambda^3}{d_{11}}}^{(\beta_{\mathrm{S}})} \overbrace{\frac{\mathrm{H}}{W}}^{(\beta_{\mathrm{G}})} . \tag{27}$$

From inspection of equation (27), the first term, β_{F}, can be considered a form-factor ratio. As N is an integer and is typically restricted to a small range of even values, there is limited tailoring capacity, therefore we focus on β_{S}, and β_{G}. The second term, β_{S}, is a ratio of stiffness properties. This term is a measure of the relative stiffness between the elastic medium and the helical lattice. Finally, β_{G}, is a geometric ratio that compares the effective thickness of the elastic medium to the width of a helical strip.

The geometric ratio is expected to lie in the middle of the range, $\beta_{\mathrm{G}} \in [0.001, 0.1]$. The permissible pseudo-ductile range, $\alpha_\Pi \in [0.51, 2.1]$, for the configuration under consideration is taken from Figure 4a. Knowledge of this range allows the permissible stiffness ratios, β_{S}, to be determined, and therefore bounded, for fixed form factors β_{F} (i.e. as a function of N), as shown in Figure 6a. It is noted that the length of the

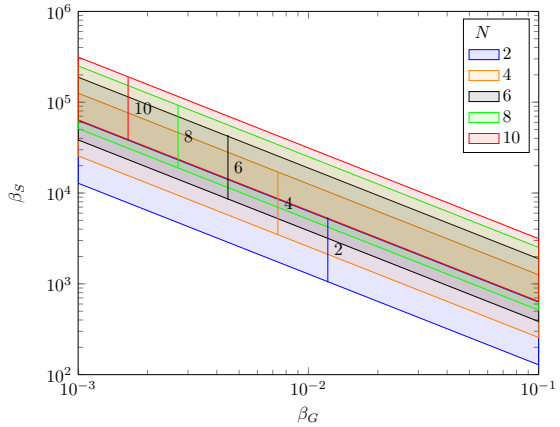

(a) Feasible regions of β_{S} as a function of β_{G} for form factors β_{F} defined by N.

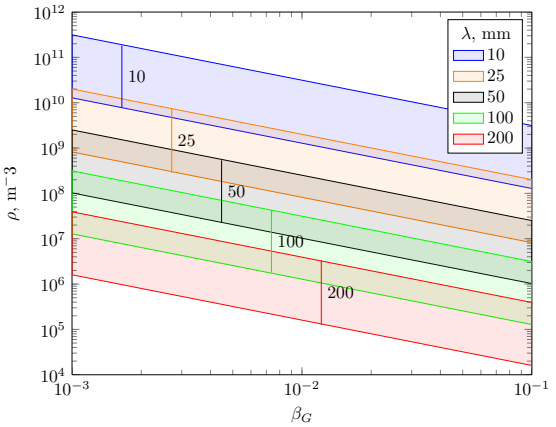

(b) Feasible ratios for ρ as determined by β_{S} as a function function β_{G} for incremental changes in unit cell λ mm, with form factor β_{F} defined by N.

Figure 6: Illustration of feasible regions of pseudo-ductility. Individual feasible regions overlap and this is indicated through the use of transparency in the shading. The width of each region is indicated through an annotated vertical line whereas the complete boundary is identified by a pair of solid coloured lines corresponding to the associated feasible region.

unit cell, Figure 2, must be sufficiently large so as to permit inclusion of all the strips comprising the helical lattice within the constraining cylinder. Due to the geometric constraint of fitting both the helical lattice and an elastic medium into a finite volume, while still permitting a full revolution of each of the helical strips within the unit cell, a restriction must be imposed on the relative size of the helical strip width such that $\lambda \gg W$. Following from the geometric assumption, it becomes necessary to consider the ratio between the bending stiffness of the helix and modulus of the elastic structure,

$$\rho = \frac{E}{d_{11}} = \frac{\beta_{\mathrm{S}}}{\lambda^3}. \tag{28}$$

While ρ is a dimensional parameter, its use allows insight into the relative magnitude that the helical lattice stiffness, d_{11}, and elastic medium, E, must possess. Importantly, ρ shows how differing λ can affect a change of several orders of magnitude in the permissible pseudo-ductile range. By selecting the range of permissible values for β_{G}, the value of β_{F} is fixed, allowing the feasible regions of ρ, as a function of β_{G}, for incremental values of λ, to be plotted. These results are shown in Figure 6b. As λ is increased the magnitude of ρ must decrease rapidly due to the cubic dependence of β_{S} on λ, equation (27). The sensitivity of β_{S} to changes in λ indicates that careful selection of the relative stiffness properties of the helix and the medium is essential in order to achieve optimal performance.

In order to maintain a value for α_{Π} that produces the pseudo-ductile behaviour seen in Figure 5 and acceptable geometries for the unit cell λ, the constraint on the ratio between d_{11} and E given by Figure 6b must be maintained. The choice of available materials has a significant effect on the feasibility of structures

such as these. Furthermore, by inspecting equation (26), the effective stress and the initial stiffness is moderated by the elastic medium's modulus E. Such a stiffness profile is expected as the initial stiffness is driven by the modulus of the elastic medium and the antagonistic behaviour of the helix is minimised. Thus the stiffness of the underlying helical structure is not exploited for initial load carrying. This unfavourable behaviour is inherent to the system in its current configuration.

The simplified configuration considered in this study limits the feasible responses to either a low stiffness-low strain configuration, or a high stiffness-high strain configuration. However, due to the potential for modifying the helical lattice, through the use of various pre-curvatures, potential improvements using optimisation methods could be realised. Furthermore, despite the limited load carrying capacity for individual structures, bundles of lattices whereby some helices contribute positively to the initial load carrying, may offer a potential mechanism to increase stiffness further. This discussion thus highlights the potential for tailoring elastic non-linear responses that are achievable from hierarchical structures comprising helical lattices embedded in an elastic medium.

5. Concluding Remarks

A preliminary analytical investigation into the behaviour of a hierarchical composite structure comprised of a composite helical lattice coupled with an elastic medium has been conducted. The potential tailorability of the non-linear elastic response has been explored with particular emphasis on the ability to introduce pseudo-ductile characteristics. Several parameters governing the feasibility of such behaviour have been identified and discussed together with the potential to further optimise the properties of such systems.

The simplified configuration considered in this study displays stiffness comparable with the elastic medium's modulus which provides some non-linear tuning capability to the elastic medium's modulus. If, however, a modulus similar in value to that of the helix material is required, further study, exploring the full extent of the design space, may yield improved performance. For example tuning of system parameters, particularly those of the helix's pre-curvature, allows for a helical lattice with increased effective stiffness to be created. Additionally, by considering bundles of differing helices, in order that some may contribute to the initial stages of load carrying, the resulting system's effective modulus may be increased. By expanding the hierarchical structural concept in this manner, the degrees of freedom available for structural tailoring are increased further. While pseudo-ductile qualities have been explored in this study the approach is applicable to more general tailoring goals.

Through exploring the behaviour of the hierarchical system using a simplified approach able to capture the system's underlying physics we are able to predict material behaviour at multiple length scales. By forming composite systems that exploit structural hierarchy it can be seen that non-linear responses may be tuned to produce desirable material characteristics. It follows that more complex systems, incorporating

helical bundles and differing materials, pre-curvatures and geometries, would allow even greater scope to tailor the response. Indeed, we have shown that by following our approach bespoke stiffness characteristics may be achievable, that has potential to be incorporated into structures constructed at larger length scales.

Acknowledgements

This work was funded under the Engineering and Physical Sciences Research Council UK (EPSRC) Programme Grant EP/I02946X/1 on High Performance Ductile Composite Technology (HiPerDuCT) in collaboration with Imperial College, London.

References

[1] G. Czél, M. Wisnom, Demonstration of pseudo-ductility in high performance glass/epoxy composites by hybridisation with thin-ply carbon prepreg, Composites Part A: Applied Science and Manufacturing 52 (0) (2013) 23 – 30.

[2] M. Jalalvand, G. Czél, M. R. Wisnom, Parametric study of failure mechanisms and optimal configurations of pseudo-ductile thin-ply ud hybrid composites, Composites Part A: Applied Science and Manufacturing 74 (2015) 123–131.

[3] M. Jalalvand, G. Czél, M. Wisnom, Mechanisms and optimal configurations of pseudo-ductile thin-ply ud hybrid composites, Composites Part A: Applied Science and Manufacturing 74 (2015) 123–131.

[4] M. Jalalvand, G. Czél, M. R. Wisnom, Damage analysis of pseudo-ductile thin-ply ud hybrid composites–a new analytical method, Composites Part A: Applied Science and Manufacturing 69 (2015) 83–93.

[5] S. Pimenta, P. Robinson, Wavy-ply sandwich with composite skins and crushable core for ductility and energy absorption, Composite Structures 116 (2014) 364–376.

[6] G. Czél, S. Pimenta, M. R. Wisnom, P. Robinson, Demonstration of pseudo-ductility in unidirectional discontinuous carbon fibre/epoxy prepreg composites, Composites Science and Technology 106 (2015) 110–119.

[7] J. Fuller, M. Wisnom, Pseudo-ductility and damage suppression in thin ply cfrp angle-ply laminates, Composites Part A: Applied Science and Manufacturing 69 (2015) 64–71.

[8] P. Fratzl, R. Weinkamer, Natures hierarchical materials, Progress in Materials Science 52 (8) (2007) 1263 – 1334.

[9] B. Bhushan, Biomimetics: lessons from nature - an overview, Philosophical Transactions of the Royal Society of London A: Mathematical, Physical and Engineering Sciences 367 (1893) (2009) 1445–1486.

[10] A. Vigliotti, D. Pasini, Mechanical properties of hierarchical lattices, Mechanics of Materials 62 (2013) 32 – 43.

[11] A. Pirrera, X. Lachenal, S. Daynes, P. M. Weaver, I. V. Chenchiah, Multi-stable cylindrical lattices, Journal of the Mechanics and Physics of Solids 61 (11) (2013) 2087–2107.

[12] X. Lachenal, P. Weaver, S. Daynes, Influence of transverse curvature on the stability of pre-stressed helical structures, International Journal of Solids and Structures 51 (13) (2014) 2479–2490.

[13] Q. Guo, A. K. Mehta, M. A. Grover, W. Chen, D. G. Lynn, Z. Chen, Shape selection and multi-stability in helical ribbons, Applied Physics Letters 104 (21) (2014) 211901.

[14] E. H. Mansfield, The bending and stretching of plates, Cambridge University Press, 2005.